International Journal of Multidisciplinary Research and Development
Online ISSN: 2349-4182 Print ISSN: 2349-5979, Impact Factor: RJIF 5.72
www.allsubjectjournal.com
Volume 3; Issue 9; September 2016; Page No. 27-42

Mineralogy and geochemistry of recent detrital sediments from Mayo Sina (Chad): Implication for the source rock location

Ekomane Emile, Bomolomo Michelle Vanessa, Zo'o Zame Philemon, Bisse Salomon Bertrant, Angtouzou Waya

Department of earth science, University of Yaounde I, P. O BOX : 812 Yaoundé/faculty of sciences, Cameroon

Abstract
Mineralogical and geochemical studies have been carried out on two alluvial profiles localised at the banks of an affluent of the Mayo Sina, South West of Chad. They were carried out in order to determine the composition of the source rock and the tectonic setting during the emplacement of the studied materials. The mineralogical and geochemical characteristics show that whole rocks, on which alluvial profiles are developed are limestone. Elemental ratios and binary diagrams suggest that the overlying materials are derive from mainly felsic rocks, with only minor contributions from a sedimentary and/or basic source. Consequently, these data suggest that, the overlying materials are not derive from the alteration of limestone, but they are transported clastic sediments and consistently suggest a continental island arc and/or active margin setting as the more probable geodynamic scenario for the deposition of the sedimentary precursors of the studied materials.

Keywords: Geochemical, mineralogy, provenance, recent detritic sediments, Chad

1. Introduction
The geochemistry of clastic sediments has been effectively used for reconstructing signature of tectonic settings, the composition of the source areas and the provenance of the sediments [43, 44, 46, 72, 64, 65, 75, 9, 8].The chemical record of clastic sedimentary rocks is potentially affected by factors such as source rock characteristics, chemical weathering, sorting processes during transport, sedimentation and post-depositional diagenesis [41, 54, 53, 20, 3]. Due to their relatively low mobility during sedimentary processes (erosion and sedimentation), some trace elements such as Zr, Hf, Y, Sc, Cr, Th, Co, La, Rare Earth Elements (REEs) and particularly TiO2 among other major elements can be used to determine geological processes, the tectonic setting and provenance of clastic sediments [18, 6, 72, 43, 44, 4, 38, 20, 3]. Louga, the study area, is located South-West of Chad, in the Mayo Kebbi Region, some kilometers from the boundary with Cameroon (Fig.1). The crystalline basement of this area is the most documented field of the Panafrican orogenesis in Chad. The first geological studies on this domain date back to the colonial period [33]. They were completed by some petrographic, geochemical and geochronological studies [34, 23, 58, 60]. These works helped to distinguish the various lithotectonic sets of this Region [33]. However, geochemical and sedimentological studies have not been carried out on the detritic deposits found in this area. The aim of this study is to determine the mineralogical and geochemical composition of these materials, with special focus on the behaviour of the REEs. The results are discussed in terms of source rocks composition and tectonic setting.

2. Materials and methods
Field works were carried out in the Louga area at the South West of Chad, during the dry season, on two alluvial profiles located on the banks of an affluent of the Mayo Sina. 12 (twelve) samples were collected from these two alluvial profiles (Fig. 2). Rs1 and Rs2 being those taken from the whole rocks.The first alluvial profile (Lo1) is located at the points of coordinate 09°08′43,4′′N and 14°24′39,8′′E, below slope, at 346 m altitude (Fig. 2a and 2b). The second alluvial profil (Lo2) is above slope, at 357 altitude and at the coordinates 09°09′10,5′′N and 14°25′02,0′′E (Fig. 2c and 2d). Samples were divided equally and prepared for granulometric, mineralogical and geochemical analyses.Grain size distribution and sample preparation were done in the Department of Earth Sciences (The University of Yaoundé I, Cameroon). The grain size distribution was accessed using the Robinson–Köln's pipetting method. After that, 20g of the bulk sediment samples were treated with cold 1 M HCl and H_2O_2 to remove organic matter. By adding sodium hexametaphosphate it deflocculated the samples. An aliquot of the bulk sediment below 2 mm grain-sized was separated in four fractions: coarse sands (2000–200µm); fine sands (200–50µm); silts (50–2µm) and clays (<2µm). Sands were separated using wet sieving. The size fractions above 50µm were determined by dry sieving. Samples were processed for mineralogical and chemical analyses at the Geoscience Laboratories (Sudbury, Canada). The mineral compositions were determined by X-ray Diffraction (XRD) analysis following two stages. Bulk and grain size sediment sampling were carried out using PAN Analytical X'PERT PRO diffractometer in the Geoscience Laboratories at 40 kV and 45 mA. This analytical instrument is equipped with a monochromator using a Co Karadiation of 1.7854 Å over a range of 2.5 to 35° 2θ with a step size of 0.05° 20/min. Oriented samples were done using a D4 Bruker Diffractometer in the University of Lille 1 (France). The goniometers were controlled by a micro-computer with the use of the PC-APD and DIFFRAC software, used to determine the optimized 2θ angles ranging from 2 to 32° and in which all clays are mainly diffracted. The obtained data are later analysed on MacDiff 4.2.5. Clay mineralogy was

determined by applying different treatments on sub-samples [71, 62]: untreated ethylene glycol and heated (550–600°C). The untreated heated and ethylene glycol sub-samples were analysed with X-ray for 30 min (2.5 s counting time). Chemical analyses were done using Rigaku RIX-3000 wavelength-dispersive X-ray fluorescence (XRF) spectrometer. Details of the XRF method are described [61]. To prepare the analysed samples for Inductively Coupled Plasma-Mass Spectrometry (ICP-MS) analysis, rock powders were digested with acid in closed beakers for lithophile trace element concentrations. The instrumental precision of almost all elements was 5% (2r) for either five or six compiled solutions where the elements were above the limit of quantification. Where the concentrations approached this limit, the error varied between 5% and 8.5% [7]. The REE data were normalized in relation to the chondrite and PAAS values [72].

3. Results

3.1 Granulometric and mineralogical characterization

The first alluvial profile (Lo1) is 430cm thick. It is located on the banks of a Mayo. This profile presents seven levels (Fig. 2a et b). From the bottom to the top, there is: very pale brown level (BM02), pale brown level (BM 03), pale yellow level (BM04), light grey level (BM05), light brown level (BM 06), very pale brown level (BM07) and brownish light level (BM08). All these levels lie on a carbonate whole rock rock (Fig. 2a et b). It is a rock that is effervescent to hydrochloric acid.

The very pale brown level is 50 cm thick, sandy silt and contains some limestone nodules, and millimetric to centimetric quartz fragments (Fig. 2a et b). The pale brown level present texture and thickness identical to those of the previous level. It contains centimetric angular quartz nodules with red brown cracks. This level is found on the roof and wall of the of the yellow level (Fig. 2a et b). The pale yellow level (70 cm) is sandy clayey silt and it is constituted of rounded quartz nodules. The light grey level (70 cm) is sandy silt and characterised by a considerable quartz content. The light brown level of 50 cm thick, is also sandy silt. This level is made up of millimetric to centimetric sub-angular quartz. The very pale brown level (30 cm) showed the same texture as the previous. It is very porous, friable and fragile. The brownish light level (20 cm) is non compact with a sandy clayey silt composition and strewed with roots of centimetric dimensions, with vertical to lateral extension.

The second alluvial profile (Lo1) is 140 cm thick. Based on the granulometric distribution, four levels, including the whole rock are distinguished (Table 1). From bottom to top, there is: pale yellow levels (BM 09), light brown (BM 10) and olive brown (BM 12). The pale yellow level is 70 cm thick and of sandy silt composition. The light brown (30 cm) is of silty composition. The following level which is 30 cm thick, corresponds to the position of the allochthoneous whole rock, of this alluvial terrace (Fig.2c et d). It is a whitish stained rock. In addition, it reacts positively to hydrochloric acid. Above this whole rock, the olive brown level of 10cm thick is observable. This level is sandy clayey silt composition and characterised by a high quartz content.

The mineralogical assemblage of the global fraction of the various samples collected from two alluvial terraces (Lo1 et Lo2) is presented in Fig. 3. The whole rock of the Lo1 alluvial profile is exclusively made up of calcite. On the other hand, that of Lo2, is composed of calcite and very little quartz (Fig. 3c). The mineralogical assemblage of the overlying materials of Lo1 alluvial profile is made up of quartz, calcite, kaolinite, smectite and muscovite (Fig. 3a). Minerals such as rutile, vermiculite, albite and microcline are in trace. This assemblage is equally the same as the materials overlying the second alluvial profile, except for the sampling BM 12 which is not exclusively composed of quartz (Fig. 3b). Fig.4 shows the presence of kaolinite and smectite in the oriented samples. Smectite is however the main mineral (content varying between 63 and 98 %) present in the clay fraction of this materials (Fig. 4; table 2). It is associated with kaolinite, illite and chlorite. This clay minerals from the fine fraction is the same in the two alluvial profiles, except in BM 12 sample. Quartz is the only non clay accessory mineral.

3.2 Geochemical characterisation

Major elements, trace elements and REE composition of analysed samples are variables and summarised in Tables 3 and 4. The enrichment of many elements is observed, in the two alluvial profiles, from whole rocks to the overlying formations. A sudden reduction of Sr is however observed (Table 4). Besides, these alluvial profiles are equally characterised by important enrichment in some elements such as Ba, Zr, V, Rb, Zn and REE (Table 4). The samples of whole rocks show moderated proportions in CaO (50.81-51.80 wt.%) and very weak in SiO_2, Al_2O_3 and Fe_2O_3 (1-3 wt.% for SiO_2, < 0.9 wt.% for Al_2O_3 and Fe_2O_3). The CaO contents reduce from whole rocks to moderately weathered materials (Table 3). This evolution contrasts with those of all other major elements. The moderated contents in CaO (50.81 wt.%) and very weak in SiO_2 (1-3 wt.%) shows that the whole rocks of the alluvial terraces are carbonate rocks. All the other major elements, except CaO, SiO_2, Al_2O_3 and Fe_2O_3, have contents lower than 1 wt.% (Table 3). Some oxydes (MnO, MgO, Na_2O, TiO2 and P_2O_5) show an identical content in the two whole rocks samples (Table 3). The alkaline content (Na_2O+K_2O) are relatively weak (0.07 à 0.12 wt.%). Whereas, the content of ($Fe_2O_3+TiO_2$) are practically similar (Table 3).

The SiO_2 contents of the overlying materials are higher than those of the whole rocks samples. Moreover, these contents increase in the same manner in the two alluvial profiles. They increase from the bottom to the top, from 50 to 87.69 wt.% (Table 3). This confirms that the fine particles are highly transported towards the bottom of the profiles [66].The high silica content of the studied samples could be attributed to their silty-sandy nature or are controlled by the sand fraction. The high concentrations in SiO_2 indicated that the sources of the detrital should have been composed entirely of quartz [1]. When these contents increase, simultaneously, those in CaO reduce, except in sample BM03. The contents in Al_2O_3 fluctuate between 4.89 and 18 wt.%. These contents are higher in the Lo1 alluvial materials (10-18 wt.%) than in those of Lo2 (4.89 -16 wt.%; Table 3). In the second alluvial profile, the contents in Fe_2O_3 and MgO increase likely, unevenly. They increase from the whole rocks to overlying formations in the alluvial profiles. The contents in MnO, TiO_2 and P_2O_5 are lower than 0.9 wt.% (Table 3). Titanium oxides is mainly concentrated in phyllosilicates [9] and is relatively immobile as compared to other elements during various

sedimentary processes and may strongly represent the source rocks [46]. The overlying materials of the two alluvial profiles show lower TiO_2 content than the post-Archean Australian average shale (PAAS; Tableau 3), which suggests more evolved (felsic) material in the source rocks [47]. The alkaline oxides (Na_2O and K_2O) have relatively high contents, those in Na_2O vary from 0.03 to 2.4 wt.% and those in K_2O from 0.85 to 2 wt.%. Besides, the contents in Na_2O of the alluvial materials of the first alluvial profile are quite higher than those of the second (Table 3). These contents in Na_2O of the alluvial materials of Lo2 alluvial profile hardly exceeds 0.12 wt.%. BM 06 is the sampling with the highest contents in Al_2O_3, Fe_2O_3, MnO, MgO, K_2O and TiO_2. Moreover and compared to the contents of other samples, they are close to those of PAAS (Table 3).

Concerning the Lo1 profile, the ratio SiO_2/Al_2O has values lower than those of Lo2. These values are likeky constant around 5 wt.%, except at the two significant points BM05 (7.61 wt.%) and BM06 (2.87 wt.%). The ratio SiO_2/Al_2O_3 are significantly high in Lo2 alluvial profile. They increase within this profile, from the bottom to the top, from 4 to17.93 wt.% (Table 3). These high values of SiO_2/Al_2O_3 is the result of an increase in the content in quartz in that area, which is the main constituent of residual materials [50]. The ratio K_2O/Na_2O in the whole rock of the second alluvial profile is about three times higher (3 wt.%) than that of whole rock of the first profile (1.33 wt.%; Table 3). Moreover, this ratio is quite higher in the Lo2 second alluvial profile (3 to 29.5 wt.%) than in the Lo1 (0.7 to 4.6 wt.%; Table 3). The decrease of this ratio is very abrupt in the Lo2 alluvial profile. The values of the Chemical Index of alteration (CIA) are practically the same in both alluvial profiles. They do not exceed 80 wt.% (Table 3). They vary from 67 to 80 wt.% for the first alluvial profile and from 47 to 79.6 wt.% for the second. Within the second profile, these values of the CIA increase from lower parts to upper parts, from 47 to 79.6 wt.% (Table 3). This fact is also observable along the profile Lo2, (from 67 to 76.5wt.%), with a significant point at 80 wt.% in the sample BM 06 (Table 3). This may be due to the strong decrease of alkaline cations (Ca, Na and K) along these alluvial profiles. In the second alluvial profile, the sum (Na_2O+K_2O) decrease lightly from the top to the bottom (Table 3). On the other hand, in Lo1 profile it varies between 0.07 and 4 wt.%. The sum Fe_2O_3 + TiO_2 is practically identical in both whole rocks (Table 3). This sum increases lightly from the whole rocks to the overlying formations of the both alluvial profiles (<7 wt.%; Table 3). The weak values of this sum are due to the strong mobility of iron causing a high depletion in these areas [68].

Among all transition metals, V has the highest concentrations (3 to 71ppm). Cr and Cu have concentrations higher than 20 ppm; meanwhile, the concentration in Ni, Co and Sc, hardly exceed 14 ppm. The concentrations lower than 0.5 ppm are those of Mo and W. The concentration of all these transition metals evolve identically, they all increase from the whole rocks to the overlying formations in both alluvial profiles (Table 4). Besides, the relatively good correlation of Cr and Ni with MgO (0.78 and 0.58; Fig.5g and h), show that the abundance of these elements seem to be controlled by chlorite.

The concentrations of *LILE* (Large-ion lithophile elements) in the analysed samples vary (Table 4). The average concentration of *LILE* is lower as compared to UCC and PAAS, except for some elements in a few samples (Table 4). The alkaline metals (Li and Rb) have relatively high concentrations. Their concentrations vary respectively from1.34 to 56.06 ppm and from 0.8 à 30.8 ppm in the alluvial profile Lo1. In the second profile, they vary between 1.97 to ~41 ppm and from ~1 to ~17 ppm (Table 4). Their increase is clearly observed from the base to the summit, along both alluvial profiles. On the other hand, the concentrations in Cs, hardly exceed 2ppm (Table 4). The Ba and Sr also have high concentrations in the first alluvial profile than in the second. The concentrations of Baryum (Ba) vary between 252 to ~800ppm. These concentrations double literally and much more from whole rocks to overlying materials (Table 4). Ba enrichment in sedimentary rocks can be considered as an indicator of detrital flux [47]. As for the Sr, it concentrations oscillate from 44 to ~1300ppm. The latter, as compare to those of Ba, abruptly decrease from whole rocks to slightly altered materials (table 4). Low Sr content generally related to low CaO content, probably due to the lack of calcic plagioclase [54, 2]. Sr is strongly correlated to CaO in the studied samples. ($r = 0.97$; Fig.5a). This strong positive correlation indicates that, the carbonates seem to be influenced by the presence of Sr. However, CaO and SiO_2 are strongly negatively correlated ($r = -0.95$; Fig. 5b). The concentrations in Be are very weak (0.09 to ~2ppm). They evolve differently from Sr. Rb and Ba are also well correlated with K_2O ($r = 0.87$ and 0.86, respectively; Fig.5e and f). These positive correlations provide evidence that K-bearing clay minerals (illite, muscovite and biotite) primarily control the abundance of these elements [43, 44, 24, 3]. This group of elements, derived from a source rich in potassium feldspar and in micas, represent the signature of the potassium felsic [43].

HFSE are preferentially partitioned into melts during crystallization and anatexis [24]. Consequently, these elements are enriched in felsic rather than mafic rocks [24, 3]. Due to their immobile characteristics, these elements are considered as a good provenance indicator, together with REEs [72, 6]. The concentration of *HFSE* (High Field Strength Elements) in the analyzed samples also vary (Table 4). Most of the sample are moderately to strongly depleted in *HFSE* as compared to UCC and PAAS (Table 4). Zr has by far the highest concentrations (from 6 to 171ppm). These concentrations are higher in the first than in the second alluvial profile. Yttrium has concentrations higher than 20 ppm; meanwhile, the concentration in Nb and Hf hardly exceed 11 ppm. The concentrations of Ta are lower than 1 ppm.

The Zr/Hf ratios in all the analysed samples (Table 4) range from 34 to 43 (average 36.67), implying that these elements are controlled by the abundance of zircons. The average ratios of Zr/Hf in studied samples are higher as compared to UCC (32.8) [72], possibly indicating that, they are the result of sediment recycling during transport [3]. The actinide concentrations the concentrations are also very weak (Table 4). They do not exceed 5ppm (0.05 à 4.74 ppm for Th and from 0.1 à 0.6ppm for U).The Th concentration is low as compared to UCC and PAAS (Table 4). All the metals, except Zn, Pb and Ga have very weak concentrations (<2ppm; Table 4).

The results of the REE analyses are summarized in Table 4. From this table, Ce and Nd have higher concentrations than the other the lanthanides (Table 4). Their concentrations are variable, weaker but nevertheless closer than those of UCC. Among the HREE, only Gd and Dy have relatively high concentrations (>3 ppm). Some lanthanides (Tb, Ho, Tm and Lu) show contents lower than 1ppm (Table 4). The REE contents vary between 11 and 136 ppm (Table 4). The smallest values were registered in whole rocks. On the other hand, the highest concentration is found in the sample BM03. LREE are approximately nine times enriched than the HREE. The relative depletion in the HREEs compared to LREEs may be due to a lower concentration of heavy minerals, for example zircon [54]. The chondrite-normalised [40] REE patterns are parallel, similar and around ten hundred times more enriched than chondrite (Fig. 6a and b; Table 4). The REE spider diagram of overlying materials are practically homogeneous in both alluvial profiles. This suggests that these materials are derive from the same parental material confirme ([50]; Fig. 6a, b). Besides, they are characterised by (i) pronounced negative anomalies in Ce (0.78 to 0.42) at the base and a positive (Ce/Ce^* = 1.41) at the summit of Lo1 alluvial profile; (ii) a negative anomaly in Ce (0.87) at the base and a positive (1.37) at the surface of the second Lo2; essentially negative Eu anomalies in the Lo2 alluvial profile (0.75 to 0.83); positive (1.11 to 1.18) and negative (0.74 to 0.81) in the first alluvial profile Lo1 (Table 4). The REE normalised to PAAS [41], of the two alluvial profile, show a geochemical signature similar to those of chondrite, despite light positive anomalies Eu (Fig. 6c-d). The variability of anomalies in Ce is a result of the redox conditions of the area [48, 50]. Meanwhile those in Eu are more related to the substitution of Sr^{2+} by l'Eu^{2+} in the feldspars. Besides, the Eu anomaly in sedimentary rocks is usually interpreted as being inherited from igneous source rocks [42; 54]. $(La/Yb)_N$ vary between 6 and 23 in the first alluvial profile, while in the second it oscillates between 7 and 15. These values show that REE fractionation decrease from whole rocks to the overlying materials. This ratio is higher in the whole rocks of the first profile (22.59) than in the second (14.67). The degree of fractionation of REE is thus strong and variable. Despite the low values, the ratio $(Gd/Yb)_N$ show similar behaviour to $(La/Yb)_N$. This ratio is lightly greater than those of PAAS and of UCC (Table 4). The ratio $(La/Sm)_N$ vary between 2 and 6 in Lo1 and between 2 and 3 in Lo2. This ratio show an antagonistic and different to the two other behaviour. It increases lightly from whole rocks to overlying materials.

Good correlations are respectively observed between the REE and Y, Zr (0.90 and 0.74; Fig.5c and d). This suggests that the REE seem to have been influenced, greatly by heavy minerals (Zircon, apatite, titanium). These minerals notably zircon, may have a significant effect on the REE spider diagrams [11, 12, 30, 13, 63].

4. Discussion

4.1 Nature of the whole Rocks

The whole rocks observed under both alluvial profiles are practically monominerals. They arecomposed of calcite. However quartz has been observed in the whole rock under the second profile. This rock contains moderate CaO contents. All the other elements have contents lower than 3%. Besides, these rocks have very high concentrations in strontium. The whole sedimentary rocks such as carbonates rarely show important concentrations of trace elements other than Sr [35]. [29] found that Sr and Mn were the only two out of ten studied trace elements that were present in greater amounts in calcite-cemented sandstone than in the non-cemented equivalent. Base on this, it is clear that these whole rocks are carbonate rocks. Moreover, they react positively with hydrochloric acid. This suggests that these carbonate rocks are limestones.

4.2 Source rocks composition and the nature of materials overlying the whole rocks

It is important to reiterate that the composition of a clastic sediment is the cumulative result of four main factors. They are: (i) the composition of source rocks, (ii) the degree of chemical weathering in the source region during the transport, (iii) the processes during transport and deposit (selection and maturity) and (iv) the mobility of elements during diagenesis [51, 36, 52, 43, 44, 67, 27, 25, 15]. The geochemical signatures of clastic sediments have been used to find out the provenance characteristics [72, 10, 15, 38, 4]. The deduction of the nature of source regions is based on: (i) the consideration of the relative abundance of detritic minerals and the major elements they contain, (ii) the distribution of REE and (iii) the relationship of compatible and incompatible elements [45]. Some elements and particularly their ratios are useful indicators of provenance as they are least affected by processes like weathering, transport and sorting. In particular, the commonly immobile elements Al, Fe, Ti, Th, Sc, Co, Cr, REEs and their ratios have been found useful [72, 69]. These elements even if mobilised do not stay for long in water and hence are almost quantitatively transferred into the sediments during weathering and transportation thus reflecting the signature of the parent materials [6, 41, 2].

First, a hypothesis on the sources of materials overlying the limestone of the two studied alluvial profiles could be put forward. It could be weathered mantle of limestones. To confirm or infirm this hypothesis, the analysis of the mineralogical and geochemical data is necessary.

The analysis of the geochemical results of whole rocks and the materials overlying them brought out many observations. In the samples of whole rocks (Rs1 and Rs2), (i) the contents in CaO are higher than 50%. On the other hand, (ii) except the two samples cited above, all the other samples show CaO contents oscillating between 0 and 12%. Whereas, they have a very high SiO_2 contents. These observations clearly show the considerable gap between the CaO and SiO_2 contents in the whole rocks and the overlying formations. Such gaps suggest a source other than the weathering of these limestones for the overlying materials. Henceforth, the earlier formulated hypothesis is questionable.

Major and trace elements, including REE contents, may supply constructive information for the provenance and the tectonic setting of clastic sediments not influenced by metamorphism, diagenesis or weathering [46, 53]. The Al and Ti exhibit low solubility during weathering and transportation processes [57, 1]. Al_2O_3/TiO_2 ratios of most clastic rocks are essentially used to infer the source rock compositions, because the Al_2O_3/TiO_2 ratio increases from 3 to 8 for mafic igneous rocks, from 8 to 21 for intermediate rocks, and from 21 to 70 for felsic igneous rocks [31, 47, 57, 1]. In most of the studied samples, except for some (BM02, BM05, BM07), the Al_2O3/TiO_2 ratio ranges from 18 to 50 (Table 3). This

suggests an intermediate to felsic rocks as the probable source rocks for these samples. This interpretation is further confirmed by the TiO_2 versus Ni and TiO_2 versus Al_2O_3 bivariate diagrams (Fig. 7 and Fig. 8). The first diagram [26] shows that the studied samples plot near the field acidic to magmatogenetic greywackes (Fig. 7). While the second diagram [56] suggests three origins for the studied samples including alkaline granites, granodiorite, and granites (Fig. 8).

Several attempts have been made to use major and trace elements as provenance indicators. [64] used major elements differentiating functions to differentiate four sources namely mafic (P1), intermediate (P2), felsic (P3) and recycled quartzose (P4). Plotting the present data in this diagram, the majority of analysed samples plotted on the P3 and P4 fields (Fig. 9). However, some samples plotted in fields P1 and P2, very closer to the limit separating these domains. P3 indicates a provenance from active continental margins (felsic source). Whereas, P4 suggests recycled continental sources associated with a passive continental margin, intracratonic sedimentary basins, and recycled orogenic provinces. According to [65], the position of the studied samples in the P4 field may also indicate that they werederived from granitic to gneissic or from a sedimentary source area similar to that observed for several recycled suites elsewhere. This was interpreted as the effect of recycling, with progressive loss of feldspar and relative increase in quartz [2]. The plot position of studied samples may therefore reflect more advanced weathering and maturation in these fluvial materials. This observation clearly indicates the little possibility of the mafic rocks as source rocks for the studied samples of the Louga [2]. Therefore, the position of studied samples indicate that they were derived from a provenance which is mainly felsic rocks, with only minor contributions from a sedimentary and/or basic sources (Fig 9).

The abundance of Cr and Ni in clastic sediments can be considered as a proxy in provenance studies [47, 3]. A low concentration of Cr and Ni indicates a felsic provenance, whereas a high content in Cr and Ni is predominantly found in sediments derived from ultramafic rocks [74, 28, 4]. The abundance in Cr and Ni (Cr > 150 ppm and Ni > 100 ppm) [28], low Cr/Ni ratios (1.3 - 1.5) and a high correlation coefficient between these two elements (r = 0.90) are indicative of ultramafic rocks in the source region [3]. The Cr (7-31) and Ni (3.6-13.9) concentrations (Table 4) in most of the studied samples are relatively low, with a significant correlation coefficient (r = 0.94) and variable Cr/Ni ratios (1.52-2.47). These low Cr and Ni concentrations in the studied samples may be not showing clear indication of source rocks composition due to carbonate dilution effects. However, low Cr and Ni abundances and high and variable Cr/Ni ratios in the studied samples do not indicate any signature of mafic or ultramafic rocks in the source region. The Cr/V ratios serve as index of the enrichment of Cr over the other ferromagnesian trace elements, whereas Y/Ni monitors have a general level of ferromagnesian trace elements (Ni) compared with a proxy for HREE (Y; [3]). The mafic to ultramafic* sources tend to have higher Cr/V (> 10*) and lower Y/Ni ratios (< 0.5*) [32, 22, 37]. The felsic rocks are characterized by Cr/V ratios lesser than 8 and Y/Ni ratios greater than 0.5 [46, 22, 1]. The Cr/V ratios range from 0.17 to 0.56 (average 0.43) and Y/Ni ratios vary from 0.9 to 5 (average 1.84; Table 4). These values are quite different from the mafic signature. They indicate a predominantly felsic lithology of the source area. Furthermore, a binary diagram of Cr/V versus Y/Ni ratios has been used to differentiate the relative contribution from ophiolitic, mafic and felsic source [32; 72; 46; 1, 3]. Plots of these studied samples show significant input from felsic sources (Fig. 10). Hence, these low Cr/V and variable Y/Ni ratios preclude any presence of the ophiolitic component in the source regions.

The most important elements used for provenance study of sedimentary materials are REE, Th, Sc, Cr [69, 24]. These elements are exclusively transported as detritical fraction of sediment, and consequently reflect the chemistry of their source area (McLennan *et al*. 1983a, b; Taylor and McLennan, 1985). Ratios such as La/Sc, Th/Sc, Th/Co, and Th/Cr are considered as suitable indicators of source rock provenance [76, 10, 14, 14, 16, 19, 69;47, 3]. They are useful in differentiating mafic from felsic sources. Sc and Co being preferentially concentrated in the former because of their compatibility with early fractionating phases. Base on that, Th and La are preferentially partitioned into melts, as incompatible elements that are associated more with the later fractionating minerals, hence having more concentration of felsic rocks [72, 69]. Thus, for the fractionated crust Th/Sc, Th/Co and La/Sc ratios are high and low for the mafic rocks. Generally, for the post Archean UCC, the ratio of Th/Sc is ~ 1, for granitic rocks it is higher and for Archean and mafic rocks it is less than 1 [70]. In this study, these ratios are compared with those of sediments derived from felsic and mafic rocks and also with UCC and PAAS values (Table 5). These comparisons show that the majority of our data are within the range of felsic to intermediate source rocks. According to [4], La/Sc and Th/Sc ratios of sediments derived from felsic rocks are always higher than those of sediments derived from mafic rocks [3]. Although some of the samples have slightly lower values of Th/Sc ratios. However, Th/Sc ratios are still much higher than those of mafic rocks and also demonstrate a felsic source. Furthermore, The Cr/Th and Th/Cr ratios of the studied samples are also within the range of felsic source rocks and are closer to those of UCC (Table 5). The Th/Co vs La/Sc plot (Fig. 11; [17]) also suggests that all studied samples were derived from felsic source rocks. In addition, Eu/Eu*, (La/Lu)n, Th/Co and La/Co ratios are significantly different in mafic and felsic source rocks and may permit constraints on the provenance of sedimentary rocks [18, 75, 14, 10, 4, 2]. The La/Co, (La/Lu)n, and Eu/Eu* ratios (Table 5) of the studied samples are compared with those in sediments derived from felsic and mafic source rocks [18,16, 19]. Such comparison indicates that the trace element ratios in this study are comparable to the range of sediments derived from felsic source rocks rather than mafic source rocks.

Besides, the Rare Earth Element (REE) are also considered to preserve the source rock composition as they carried almost entirely by the detrital component [72, 75, 69]. They are useful in differentiating between the felsic and mafic source. Felsic rocks contain higher LREE/HREE ratios and negative Eu anomalies. In contrast, mafic rocks generally contain lower LREE/HREE ratios with little or no Eu anomalies [14]. The positive Eu anomalies are generally found in Precambrian rocks [tonalite-tronjhemite-gneiss (TTG), granodiorite, and quartz diorite]. The TTG rocks exhibit very high LREE/HREE ratios and no or small positive Eu anomalies, and the positive anomaly resulted from hornblende-melt

equilibria [47]. The positive Eu anomaly was also related to feldspars, which together with quartz, are the main components of the coarse sand fraction [70; 69; 49]. In this study, chondrite-normalized REE patterns for studied samples characterized by high LREE/HREE ratio (7.06-11.67, average 9.40), almost flat HREE patterns, fractionated REE patterns with (La/Yb) n varying from 6.6 to 19.2 and little but variable negative Eu anomalies (average 0.93). Generally, these characteristics present the felsic source rocks of the Louga's materials.

The Th/Sc ratios were used as an indicator of chemical differentiation, hence, to infer compositional heterogeneity of the sources [10; 3]. The Zr/Sc ratios were used as an index of sediment recycling in the source region [46]. Moreover, Th/Sc ratios higher than 0.8, if coupled with higher values of Zr/Sc, will probably indicate input from mature and/or recycled sources. All the studied samples, when plotted into the Th/Sc versus Zr/Sc binary diagram (Fig. 12) show a positive slope. Their Th/Sc and Zr/Sc ratios are similar to the upper continental crust and felsic volcanic rocks [46] confirming their source from a felsic source area (Fig. 11).

In summary, chemistry has helped specify the composition of the source. Indeed, the use elements relatively immobile such as (La, Th, Sc…), the ratios of La/Sc, Th/Sc, Cr/Th, Th/Co, La/Co, $(La/Lu)_N$, the binary diagram of TiO2 vs Ni, Cr/V vs Y/Ni, Th/Sc vs Zr/Sc and the REE distribution patterns including Eu/Eu* of the analysed materials indicate that (i) they were derived from mainly felsic source rocks, with only minor contributions from basic sources. This information rejects the hypothesis earlier formulated regarding the mantle, and rather confirms that these materials are clastic alluvial deposits discharged on the limestones during variations of the flow of the Mayo.

4.3 Tectonic Setting

The geochemical compositions of major and trace elements of sedimentary rocks have been extensively used to differentiate tectonic settings of sedimentary basins [5, 64, 56, 3].

[64] have developed a bivariate tectonic discriminator using SiO_2 and K_2O/Na_2O ratios to determine the tectonic setting of terrigenous sedimentary rocks. This plot does not discriminate between the oceanic island arc and continental margin arc settings [5], which plotted together in the active continental margin field. Moreover, it does not discriminate between the Recycled Orogen and the Continental Block sources [21], which plotted together in the passive margin field [59]. The major element plots of this study show that the studied samples fall within the active and passive continental margins, indicating that both margins are the main sources of the Louga materials (Fig. 13a). Both SiO_2 and K_2O/Na_2O values increase from volcanic arc to active-continental-margin to passive margin settings that signify continentally derived sediments differentiated by high SiO_2 and low Na_2O [2]. Low Na_2O/K_2O and SiO_2 content in some samples have shifted these points into the active-continental margin field. Therefore, the tectonic discrimination diagrams are to be used with restrictions [20]. The samples that plot within the passive margin field are dominated by rich quartz sediments and fall in active continental margin field, reflecting more weathered material [64, 20]. The former corresponds to the group that plot in the P4 field in Fig. 9. This suggests that they were derived from a cratonic interior or a recycled orogenic terrain.

The Lanthanum-Thorium-Scandium plot [5] provides discrimination between different tectonic settings: oceanic island arc (A), continental island arc (B), active continental margin (C), and passive margin (D); note that B and C are separated here, in contrast to [64]. Moreover, Arc fields are separated moderately well, but passive margin and active continental margin fields overlap [59]. In the ternary plot of La–Th–Sc, the studied samples fall in the field of continental island arcs (Fig. 13b).

Finally, our results indicate that the studied materials were deposited in a tectonically active continental margin and/or a continental island arc setting and are in agreement with the tectonic history of the Mayo Kebbi Region.

5. Tables and Figures

Table 1: Granulometric composition (percentages %) of alluvial materials of studied samples.

	Alluvial Profil Lo1							Alluvial Profil Lo2		
	BM02	**BM 03**	**BM 04**	**BM 05**	**BM 06**	**BM 07**	**BM 08**	**BM 09**	**BM 10**	**BM 12**
Coarse sand	51.40	57.64	46.03	62.77	13.68	59.47	42.41	36.21	23.80	40.33
Fine sand	13.78	14.43	10.63	11.61	36.37	13.58	11.17	5.04	22.54	13.65
Silt	24.29	13.60	16.34	17.74	35.50	15.79	11.66	20.13	36.60	15.06
Clay	10.53	14.34	27.00	7.88	14.45	11.16	34.76	38.62	17.07	30.96
Total	100.00	100.00	100.00	100.00	100.00	100.00	100.00	100.00	100.00	100.00

$200 < \Phi < 2000$ µm (coarse sand); $200 < \Phi < 50$ µm (fine sand); $50 < \Phi < 20$ µm (coarse silt); $20 < \Phi < 2$ µm (fine silt); $\Phi < 2$ µm (clay).

Table2. Mineralogic composition of fraction <2µm alluvial materials of the studied samples (%).

	Alluvial Profil Lo1								Alluvial Profil Lo2			
	Rs1	**BM02**	**BM03**	**BM04**	**BM05**	**BM06**	**BM07**	**BM08**	**BM09**	**BM10**	**Rs2**	**BM12**
Smectite	98	96	98	96	96	97	97	96	91	95	98	63
Illite	1	2	1	2	3	2	2	2	1	1	1	2
Kaolinite	1	2	1	2	1	1	1	2	8	4	1	30
Chlorite	–	–	–	–	–	–	–	–	–	–	–	5
Accessory												Quartz

Table3: Major element composition (wt. %) and element ratios of studied materials.

		Alluvial Terrasses													
	d.l	Alluvial Profil Lo1								Alluvial Profil Lo2					
		Rs1	BM 02	BM 03	BM 04	BM 05	BM 06	BM 07	BM 08	BM 09	BM 10	Rs2	BM 12	PAAS	UCC
SiO_2	0.04	1.30	66.36	69.36	67.30	78.67	52.29	70.85	73.48	50.86	51.70	3.04	87.69	62.80	65.67
TiO_2	0.01	0.01	0.18	0.71	0.33	0.09	0.74	0.15	0.25	0.50	0.51	0.01	0.17	1.00	0.50
Al_2O_3	0.02	0.37	13.52	13.13	14.45	10.34	18.25	13.63	12.47	12.31	16.08	0.71	4.89	18.90	15.12
Fe_2O_3	0.01	0.09	1.35	2.74	2.56	0.63	6.52	1.18	1.85	3.65	4.20	0.12	1.49	6.50	4.98
MnO	0.002	0.02	0.02	0.04	0.03	0.07	0.12	0.02	0.03	0.06	0.05	0.02	0.03	0.11	0.08
MgO	0.01	0.16	0.90	0.93	1.16	0.74	2.54	1.01	0.77	0.86	1.48	0.16	0.20	2.20	2.19
CaO	0.006	50.81	4.08	2.13	1.72	1.10	1.82	1.49	1.01	12.50	7.73	51.80	0.28	1.30	4.18
Na_2O	0.02	0.03	1.00	2.28	1.42	1.73	0.47	2.40	1.09	0.06	0.06	0.03	0.12	1.20	3.88
K_2O	0.01	0.04	1.61	1.78	1.66	1.70	2.19	1.65	1.73	1.25	1.77	0.09	0.85	3.70	3.38
P_2O_5	0.002	0.02	0.05	0.36	0.14	0.15	0.11	0.04	0.02	0.12	0.21	0.02	0.02	0.16	-
LOI	0.05	46.28	9.80	5.20	7.90	3.89	13.96	5.86	6.64	17.28	15.46	43.28	3.50	-	-
Total	-	99.13	98.87	98.66	98.67	99.11	99.01	98.28	99.34	99.45	99.25	99.29	99,24	97.87	99.98
CIA	-	-	66.90	67.96	75.06	69.54	80.29	71.10	76.50	47.13	62.71	-	79.64	75.30	<50
SiO_2/ Al_2O_3	-	3.51	4.91	5.28	4.66	7.61	2.87	5.20	5.89	4.13	3.22	4.28	17.93	3.32	4.34
K_2O/ Na_2O	-	1.33	1.61	0.78	1.17	0.98	4.66	0.69	1.59	20.83	29.50	3.00	7.08	3.08	0.87
$Na_2O+ K_2O$	-	0.07	2.61	4.06	3.08	3.43	2.66	4.05	2.82	1.31	1.83	0.12	0.97	4.9	7.26
$Fe_2O_3+TiO_2$	-	0.10	1.53	3.45	2.89	0.71	7.26	1.33	2.10	4.15	4.71	0.13	1.66	7.5	5.48
Al_2O_3/ TiO_2	-	37,00	75,11	18,49	43,79	114,89	24,66	90,87	49,88	24,62	31,53	71,00	28,76	18.90	30.24

Rs1 and Rs2: Whole rocks; for other acronyms, see Table 1; d.l.: detection limits; LOI: loss on ignition (1000°C); CIA = [Al_2O_3 / (Al_2O_3+ CaO +Na_2O+K_2O)] * 100 [54]. PAAS [72].

Table 4: Trace and rare-earth elements composition (ppm) of studied materials.

	d.l	Rs1	BM 02	BM 03	BM04	BM05	BM 06	BM07	BM08	BM 09	BM10	Rs2	BM12	PAAS	UCC
Cr	3	3	7	12	17	5	31	7	15	24	24	3	13	110.0	35.0
V	0.8	5.5	16.9	71.2	30.6	12.1	65.6	15.2	29.8	59	49.4	3.7	29.3	150.0	60.0
Co	0.13	0.58	2.75	5.26	4.93	2.18	11.88	2.83	4.82	8.32	8.18	0.7	5.48	23.0	10.0
Ni	1.6	7.7	4.1	5.2	8	3.6	13.9	4.6	7.5	12.6	9.7	6.7	5.8	55.0	20.0
Sc	31.1	< 1.1	3.4	5.8	5	2.1	10.6	3	4.3	6.2	8.1	1.3	2.7	16.0	11.0
Cu	1.4	2	6.7	6.6	10.7	4.7	27.9	4.8	9.2	14.8	15.5	2.2	4.5	50.0	27.0
W	0.05	< d.l	0.07	0.27	0.17	0.05	0.41	0.07	0.19	0.32	0.29	< l.d	0.16	2.7	2.0
Mo	0.08	0.08	0.09	0.3	0.14	0.11	0.16	0.1	0.15	0.23	0.17	0.09	0.22		
Rb	0.23	1.34	19.89	33.4	29.63	21.67	56.06	23.62	32.74	34.2	40.98	1.97	16.13	160.0	112.0
Cs	0.01	0.04	0.36	0.49	0.91	0.36	1.98	0.43	0.72	0.97	1.23	0.05	0.42	5.16	3.7
Ba	0.8	307.70	603.20	770.9	633.5	800.6	635.9	723.3	687	438	530.9	252	369.8	650.0	550.0
Sr	0.6	1329.7	153.8	234.1	187.9	184	136.8	261.2	160.6	167.2	97.7	1151.9	44.3	200.0	350.0
Li	0.4	0.8	11.30	7.6	15	6.7	30.8	7.7	10.4	14.8	17.3	0.9	5.4		
Be	0.04	0.13	0.92	1.47	1.84	0.86	2.1	0.92	1.37	1.35	1.64	0.09	0.55		3.00
Zr	6	6	40	171	57	31	144	48	95	115	151	< d.l	112	210.0	190.0
Hf	0.14	< d.l	1.17	3.95	1.61	0.87	4.02	1.35	2.57	3.11	4.18	<d.l	3.05	5.00	5.8
Y	0.05	1.31	5.06	23.76	10.3	18	12.54	4.32	7.7	12.55	15.11	1.46	5.34	27.0	22.0
Nb	0.03	0.16	1.46	11.16	4.44	1.01	8.24	2.09	4.18	6.08	6.42	0.28	2.97	1.90	25.0
Ta	0.02	< d.l	0.09	0.73	0.32	0.07	0.52	0.16	0.3	0.38	0.43	<d.l	0.23	-	2.2
Th	0.02	0.06	0.96	3.29	2.49	0.77	4.74	0.85	2.08	3.83	3.32	0.05	2.18	14.60	10.7
U	0.01	0.5	0.16	0.6	0.35	0.19	0.52	0.13	0.45	0.56	0.55	0.26	0.44	3.10	2.8
Zn	7	< d.l	20	30	32	14	100	20	22	34	60	< d.l	8	85.0	67.0
Ga	0.04	0.48	13.95	14.03	15.8	10.44	23.83	13.52	13.5	14.15	18.92	0.76	5.61	20.0	17.0
Pb	0.6	< d.l	5.1	8.3	7.5	5.3	11.4	5.7	7.6	7.8	8.5	0.7	5.4	20.0	17.0
Sn	0.16	< d.l	0.4	1.48	0.81	0.21	1.61	0.48	0.62	1.22	1.18	< d.l	0.47		5.50
Tl	0.005	0.01	0.07	0.13	0.12	0.09	0.23	0.09	0.13	0.15	0.19	0.01	0.09		
Zr/Sc			11.76	29.48	11.4	14.76	13.58	16	22.09	18.55	18.64		41.48	13.13	17.27
Zr/Hf	-	-	34.19	43.29	35.40	35.63	35.82	35.56	36.96	36.98	36.12	-	36.72	42.00	32.76
Cr/Ni	-	-	1.71	2.31	2.13	1.39	2.23	1.52	2	1.9	2.47	-	2.24	2	1.75
Cr/V	-	-	0.41	0.17	0.56	0.41	0.47	0.46	0.5	0.41	0.49	-	0.44	0.73	0.58
Y/Ni	-	-	1.23	4.57	1.29	5	0.9	0.94	1.03	1	1.56	-	0.92	0.50	1.1
REE	-														
La	0.04	2.66	5.3	22.55	18	24.41	29.22	11.02	8.72	20.56	14.49	2.16	7.15	38.20	30.00
Ce	0.12	4.88	11.93	53.25	37.1	32.61	45.33	8.82	26.18	42.29	26.65	4.57	20.26	79.60	64.00
Pr	0.01	0.85	1.61	6.93	4.68	4.41	7.32	2.39	2.33	5.14	3.79	0.63	1.78	8.83	7.10
Nd	0.06	3.96	6.74	29.45	18.35	17.21	27.85	8.9	9.24	20.34	16.04	2.5	6.74	33.90	26.00
Sm	0.012	0.82	1.48	6.07	3.15	2.74	4.87	1.44	1.94	3.76	3.41	0.56	1.26	5.55	4.50
Eu	0.003	0.18	0.51	1.53	0.85	0.95	1.27	0.45	0.57	0.89	0.99	0.13	0.31	1.08	0.88
Gd	0.009	0.67	1.17	5.4	2.38	2.92	3.53	1.06	1.53	3.01	3.1	0.5	1.02	4.66	3.80

Tb	0.002	0.08	0.17	0.76	0.31	0.4	0.48	0.14	0.24	0.42	0.43	0.06	0.15	0.77	0.64
Dy	0.009	0.4	0.97	4.59	1.86	2.45	2.62	0.77	1.44	2.36	2.59	0.33	0.93	4.68	3.50
Ho	0.003	0.06	0.19	0.87	0.34	0.49	0.48	0.14	0.28	0.43	0.5	0.06	0.19	0.99	0.80
Er	0.007	0.16	0.52	2.49	0.96	1.42	1.35	0.41	0.86	1.23	1.43	0.14	0.57	2.85	2.30
Tm	0.002	0.02	0.08	0.36	0.14	0.19	0.2	0.06	0.13	0.18	0.21	0.02	0.09	0.41	0.33
Yb	0.009	0.08	0.51	2.32	0.91	1.16	1.33	0.39	0.87	1.18	1.36	0.1	0.61	2.82	2.22
Lu	0.002	0.01	0.08	0.33	0.14	0.17	0.21	0.06	0.13	0.18	0.22	0.01	0.09	0.43	0.32
REE	-	14.83	31.26	136.73	89.17	91.53	126.06	36.05	54.2	101.97	75.21	11.77	41.15	184.77	
LREE	-	13.35	27.57	119.78	82.13	82.33	115.86	33.02	48.98	92.98	65.37	10.55	37.5		127.10
HREE	-	1.48	3.69	16.95	7.04	9.2	10.2	3.03	5.22	8.99	9.84	1.22	3.65		9.18
LREE/ HREE	-	9.02	7.47	7.06	11.67	8.95	11.36	10.90	9.38	10.34	6.64	8.65	10.27		
Ce/Ce^*	-	0.785	0.988	1.03	0.98	0.76	0.75	0.42	1.41	1	0.87	0.947	1.37	1.02	1.03
Eu/Eu^*	-	0.74	1.18	0.81	0.95	1.02	0.93	1.11	1.01	0.81	0.93	0.75	0.83	0.63	0.71
$(La/Yb)_N$	-	22.59	7.06	6.6	13.44	14.3	14.92	19.2	6.81	11.84	7.24	14.67	7.96	9.15	9.21
$(La/Sm)_N$	-	2.03	2.24	2.32	3.57	5.56	3.75	4.78	2.81	3.41	2.65	2.41	3.54	4.33	4.19
$(Gd/Yb)_N$	-	6.78	1.86	1.88	2.12	2.04	2.15	2.2	1.42	2.06	1.84	4.05	1.35	1.34	1.40

Table 5: Range of elemental ratios of studied samples compared to the ratios in similar fractions derived from felsic rocks, mafic rocks, upper continental crust, and Post-Archean Australian Shale.

Elemental ratio	Range of Louga's samples[1]		Range of sediments[2]		UCC[3]	PAAS[3]
	Profil alluvial Lo1 (t=7)	Profil alluvial Lo2 (t=3)	Felsic rocks	Mafic rocks		
La/Sc	1,56-11,62	1,79-3,32	2.5 - 16.3	0.43 - 0.86	2.21	2.4
Th/Sc	0,28-0,57	0,41-0,81	0.84 - 20.5	0.05 - 0.22	0.79	0.9
Th/Cr	0,12-0,27	0,14-0,17	0.13 - 2.7	0.018 - 0.046	0.13	0.13
Cr/Th	3,65-8,24	5,96-7,23	4.00 – 15	25 – 500	7.76	7.53
Th/Co	0,30-0,63	0,40-0,46	0.67 - 19.4	0.04 - 1.4	0.63	0.63
La/Co	1.81-11.20	1.30-2.47	1.8-13.8	0.14-0.38	3	1.66
$(La/Lu)_n$	6.88-19.06	6.84-11.85	3.00-27.00	1.10-10.00	/	/
Eu/Eu*	0.81-1.18	0.81-0.93	0.40-0.94	0.71-0.95	0.71	0.63

[1] This study; [2] [14, 16, 18, 19]; [3] [72]. *t* = number of samples; where subscript n indicates normalization to chondrite.

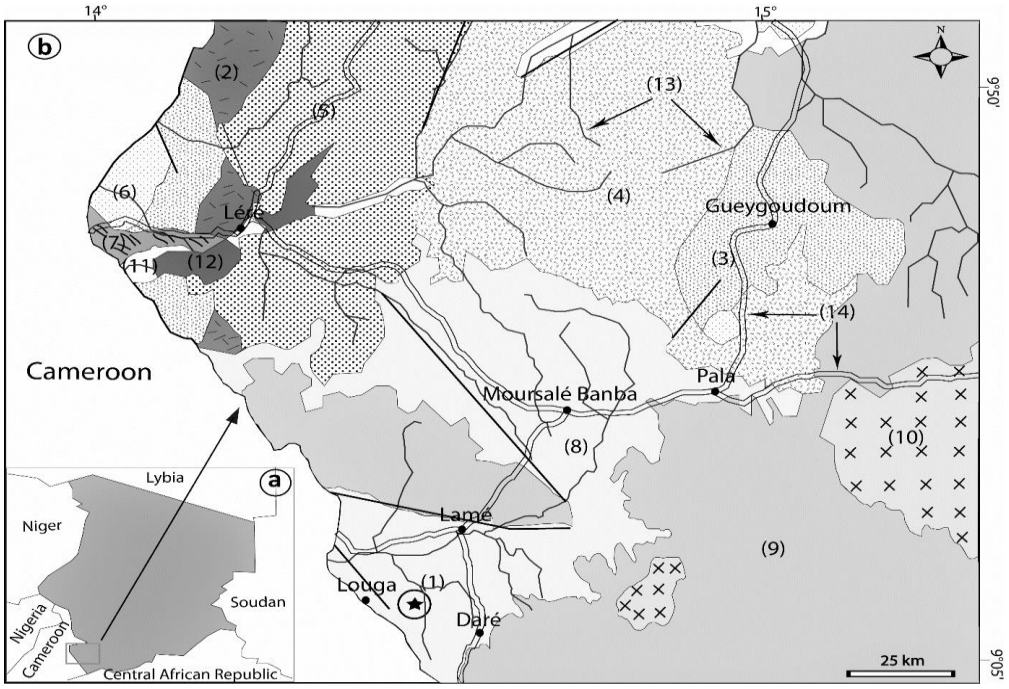

Fig 1. Location and geological map of the study area :(a) Location of the study area in the south west of Chad; (b) Geological map of the west Mayo Kebbi Region [74, 33] 1. Study site; 2. Gabbro/Gabbro-diorite; 3. Metavolcosediments; 4. Magmatic complex of chutes de Gauthiot; 5. Magmatic complex of Léré; 6. Post tectonic granites (Precambrian); 7. Lower Cretaceous; 8. Upper Cretaceous; 9. Tertiary II; 10. Tertiary I; 11. Quaternary; 12. Lake; 13. Water curse; 14. Road.]

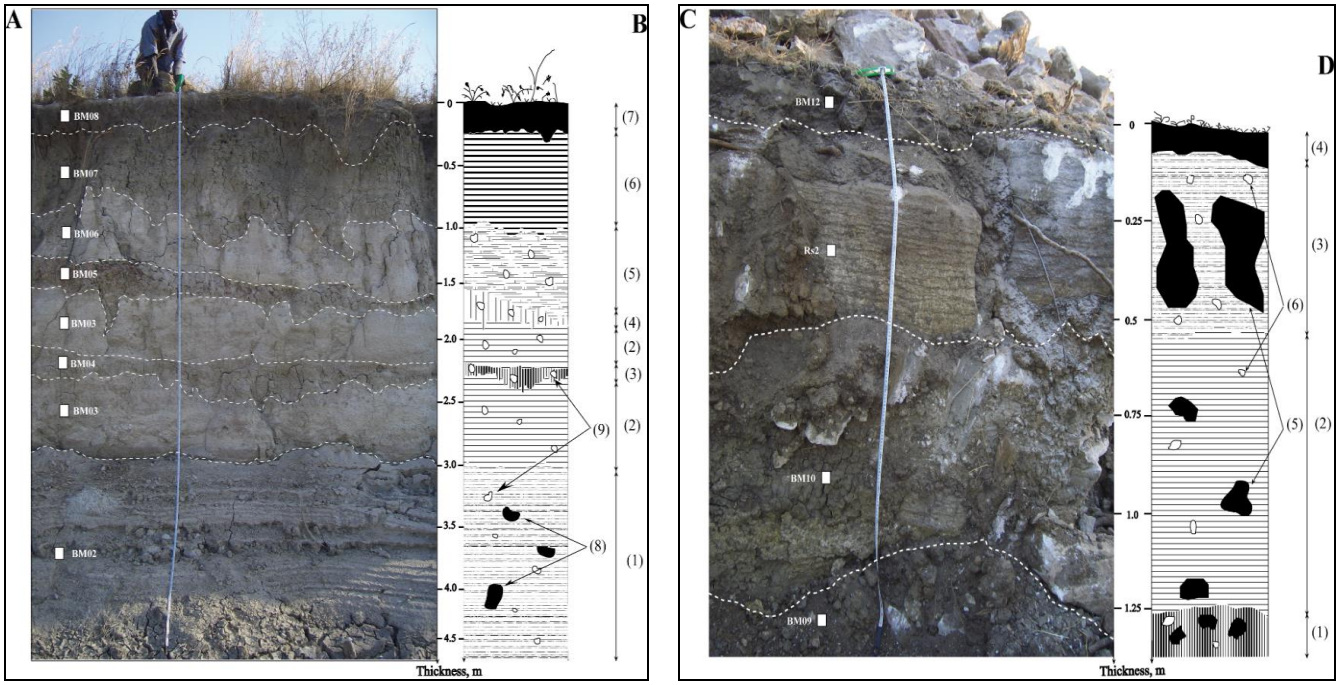

Fig 2: (A), (C): Vertical Section of the two alluvial profiles localized on the banks of an affluent (stream) of Mayo Sina with collected samples (white public gardens) in the different sedimentary layers. B: Macroscopic organization of the weathering profile Lo1: (1) very pale brown level; (2) pale brown level; (3) pale yellow level; (4) light grey level; (5) light brown level; (6) very pale brown level; (7) brownish light level ; (8) calcarous nodules; (9) fragments of quartz. D : Macroscopic organization of the weathering profile Lo2: (1) pale yellow levels; (2) light brown levels; (3) Whole rock; (4) olive brown levels; (5) fragments of calcarous rocks; (6) fragments of quartz.

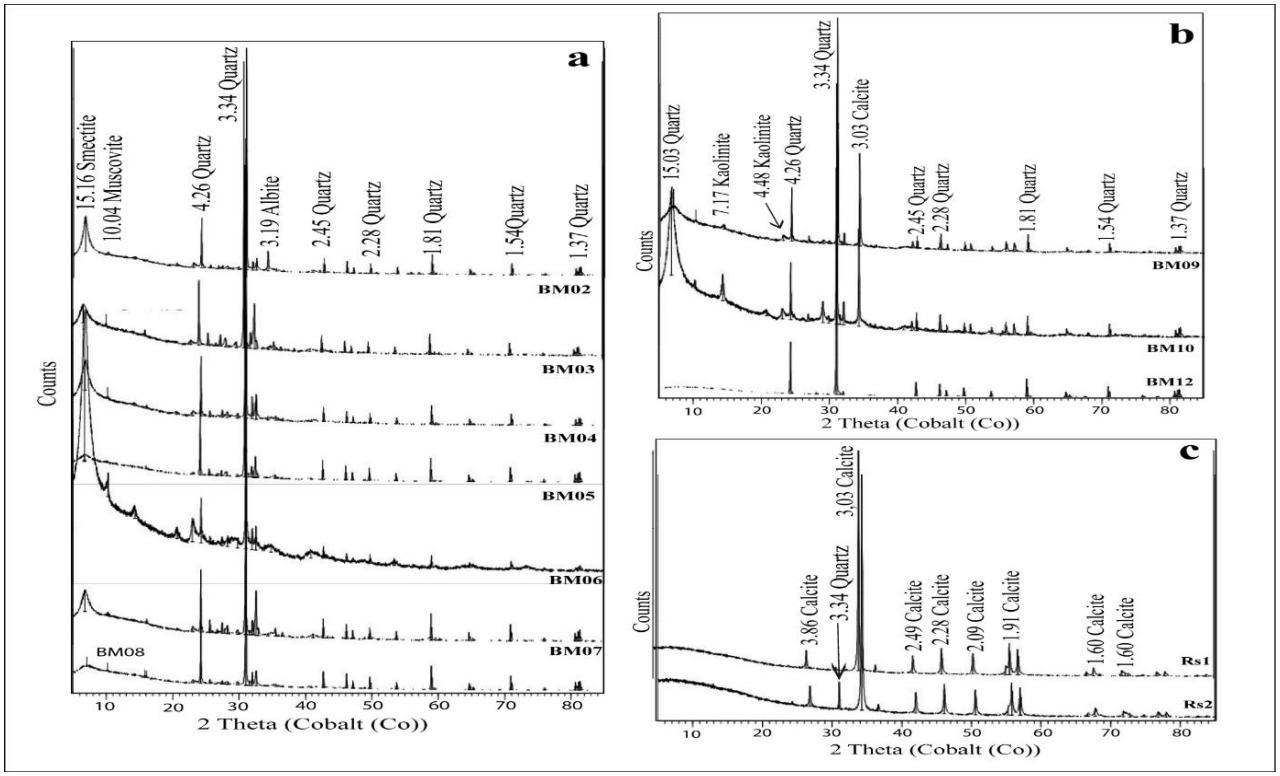

Figure 3. X-ray diffraction spectra characteristic of the studied samples: (a) BM02 to BM08 from Lo1 alluvial profile; (b) BM09 to BM12 from the Lo2 alluvial profile; (c) Rs1 and Rs2 from both alluvial profile.

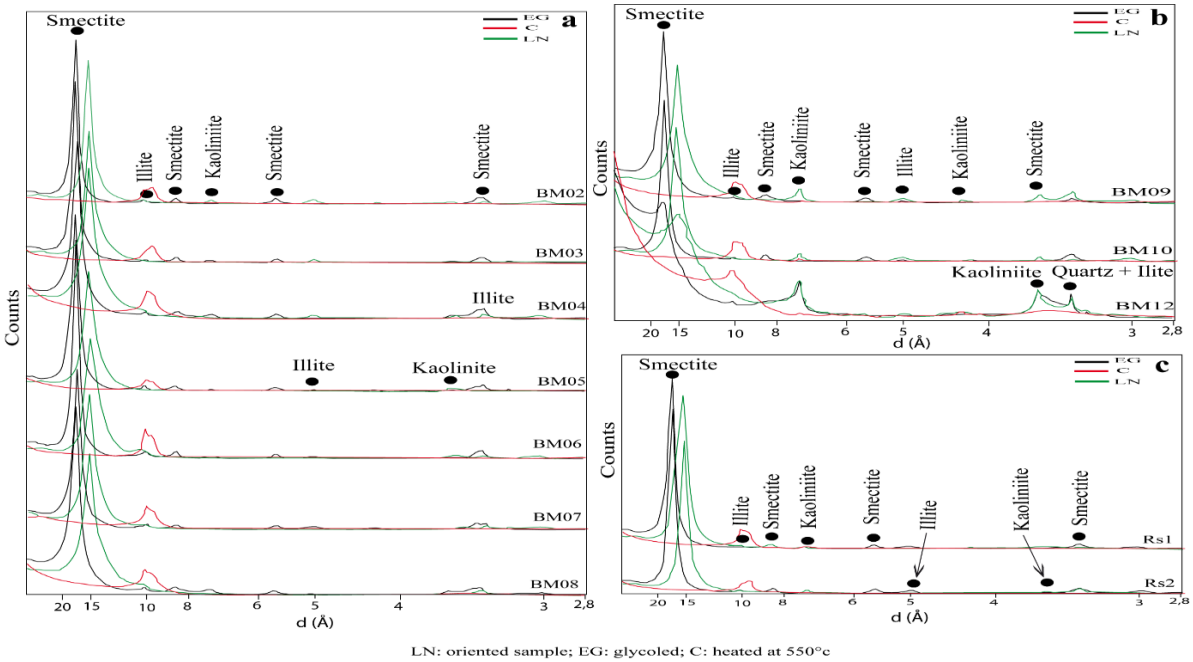

Fig 4: X-ray diffraction spectra characteristic of clays materials after specific treatments: (a) BM02 to BM08 from Lo1 alluvial profile; (b) BM09 to BM12 from the Lo2 alluvial profile; (c) Rs1 and Rs2 from both alluvial profile respectively.

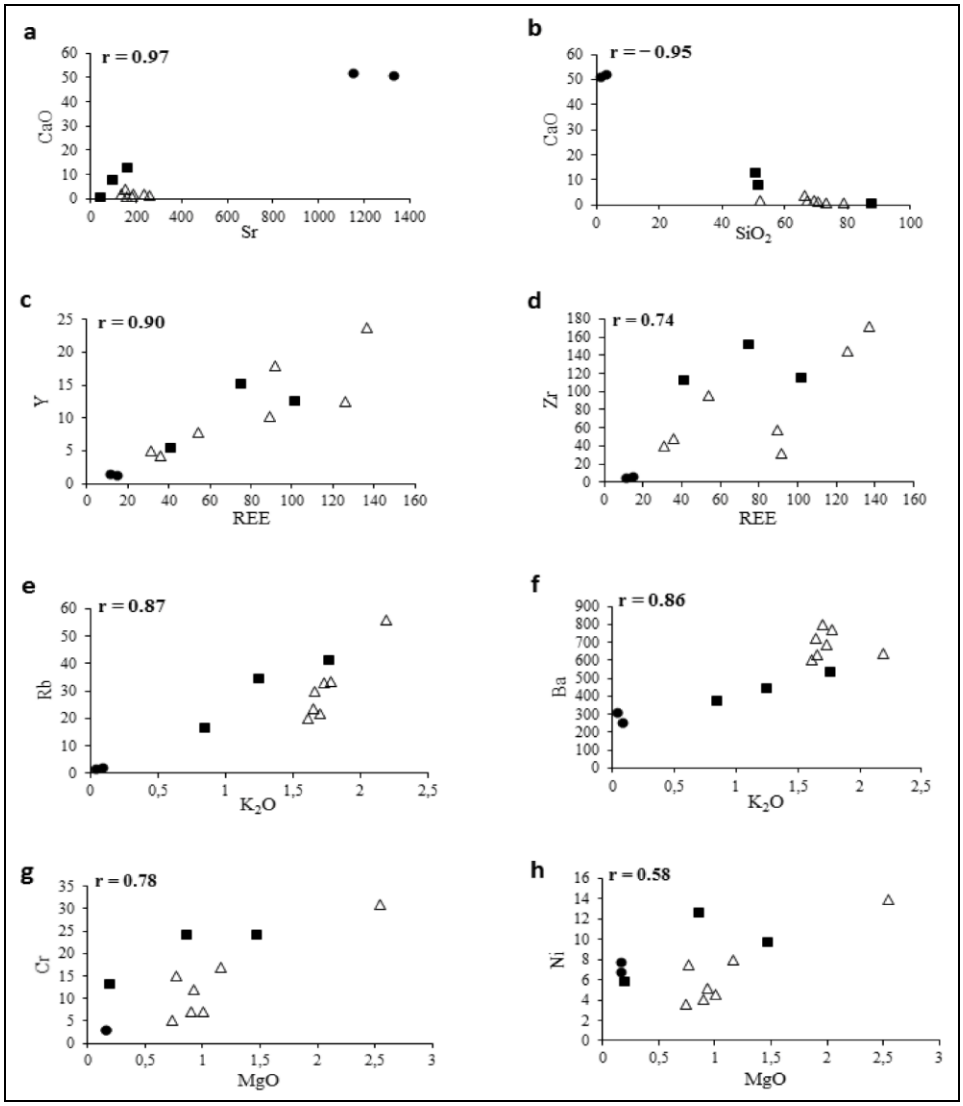

Fig 5. Harker variation diagrams of selected elements

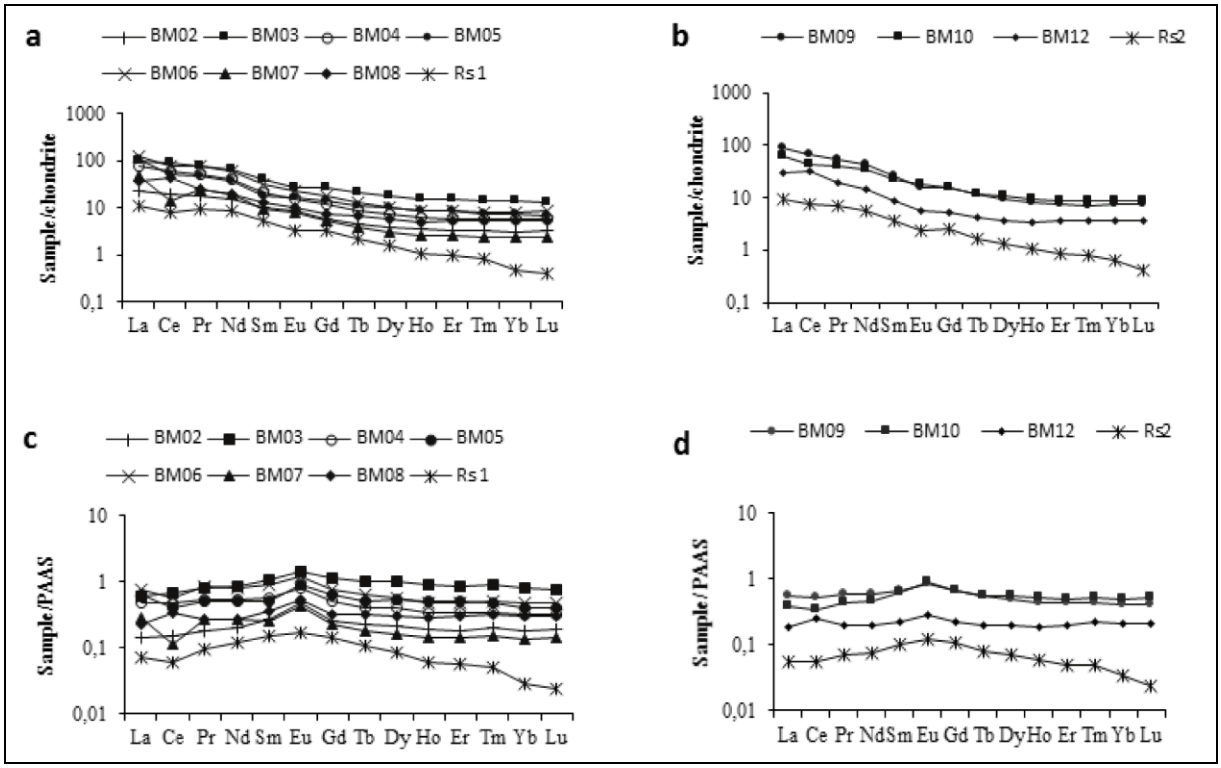

Fig 6: Spectra characteristics of rare earth elements of sampled materials: alluvial profiles Lo1 (a) and Lo2 (b) Chondrite normalization [40]; (c) and (d) PAAS [41]. PAAS: Post-Archaean Australian Shale; REE: Rare Earth Elements.

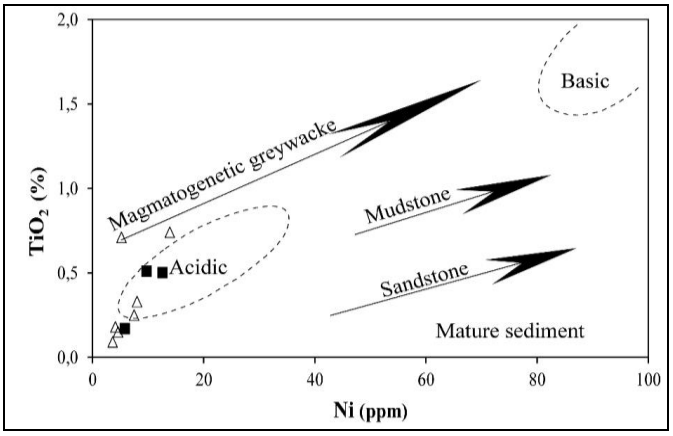

Fig 7: TiO2 versus Ni bivariate plot for studied samples [26].

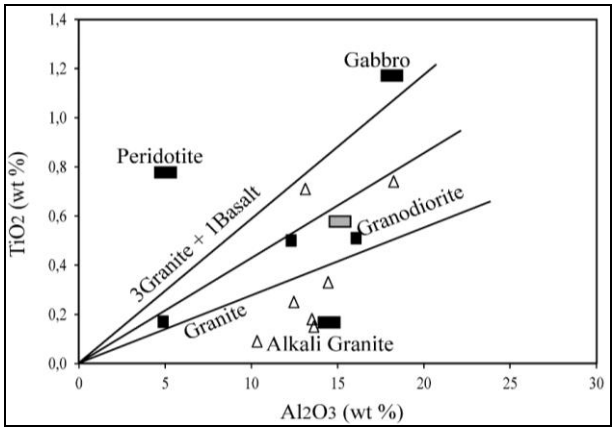

Fig 8: TiO_2 versus Al_2O_3 bivariate diagrams for studied samples [56]

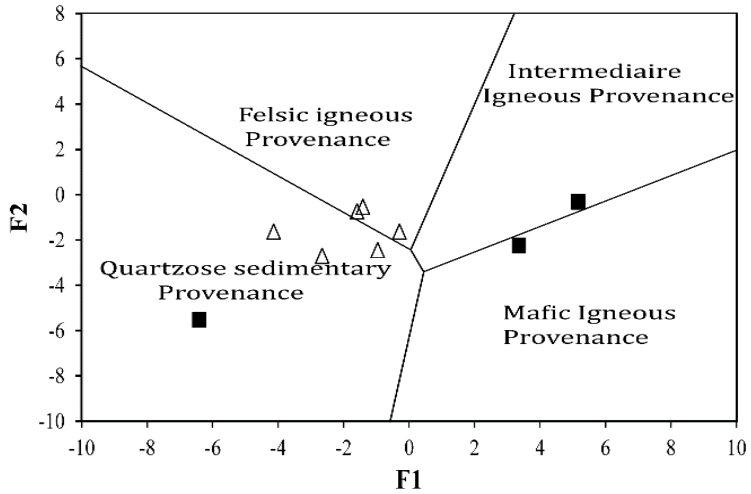

Fig 9: Plot of analysed samples on the discriminant function diagram [64].

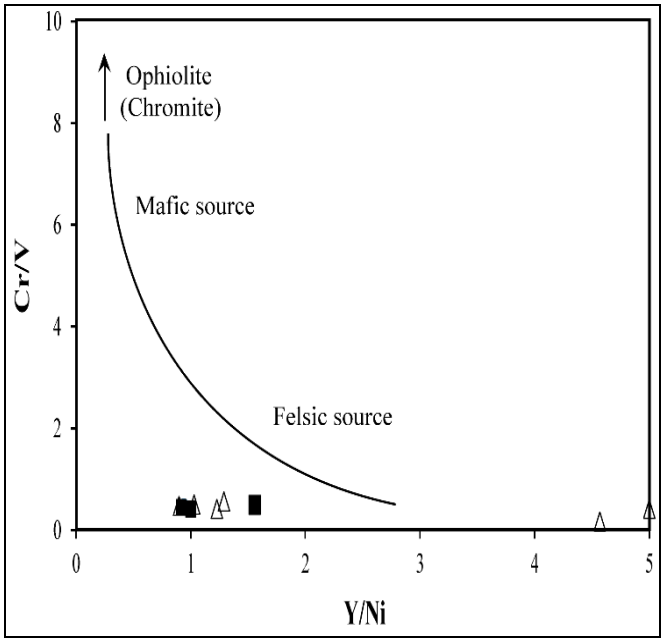

Fig 10: Analyzing the provenance by using relations of Cr/V versus Y/Ni [32]. Curve model between granite and ultramafic end members. Ultramafic rocks have very low Y/Ni and high Cr/V ratios. Arrow indicates the direction of the mafic-ultramafic source end-end members.

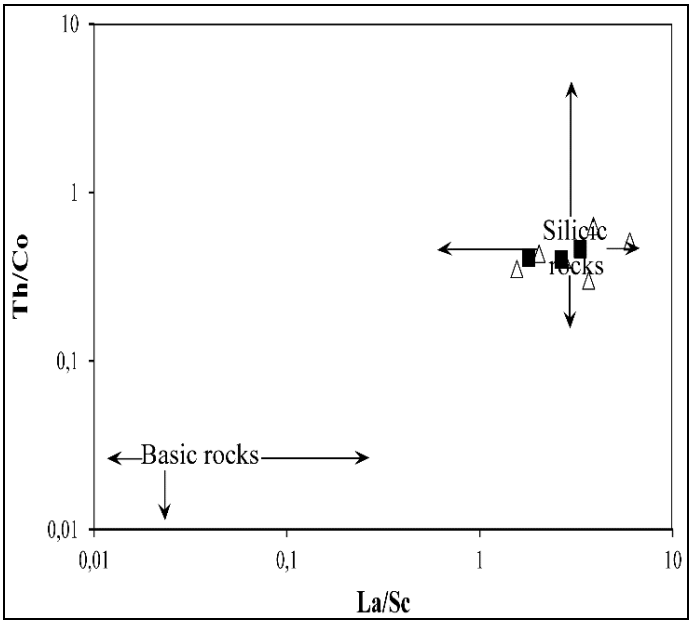

Fig 11: Th/Co versus La/Sc diagram for the studied samples [17].

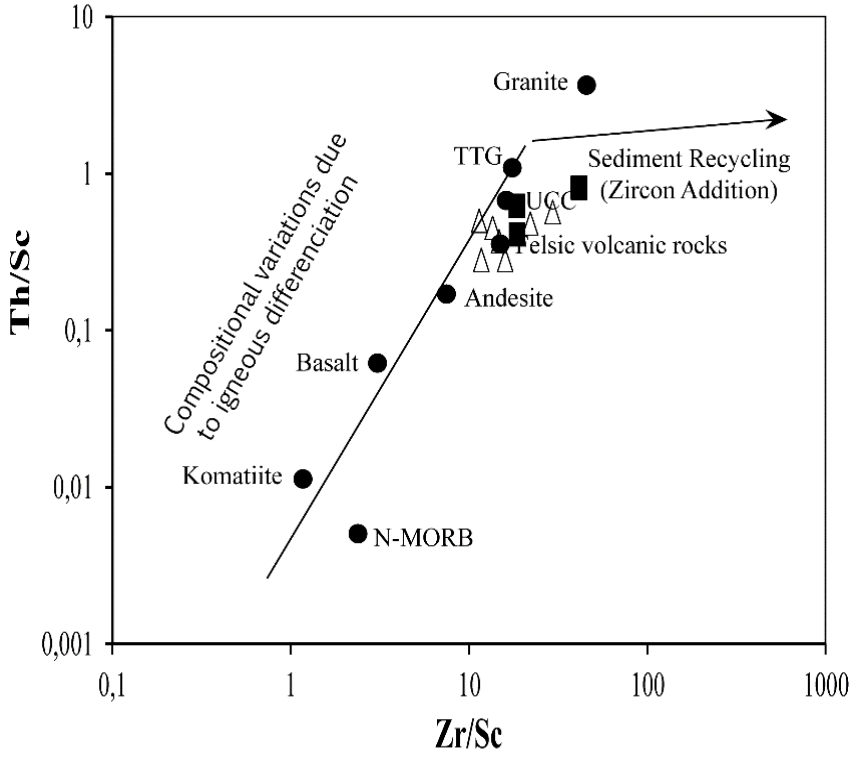

Fig 12: Th/Sc versus Zr/Sc Plot [46] for the studied samples.

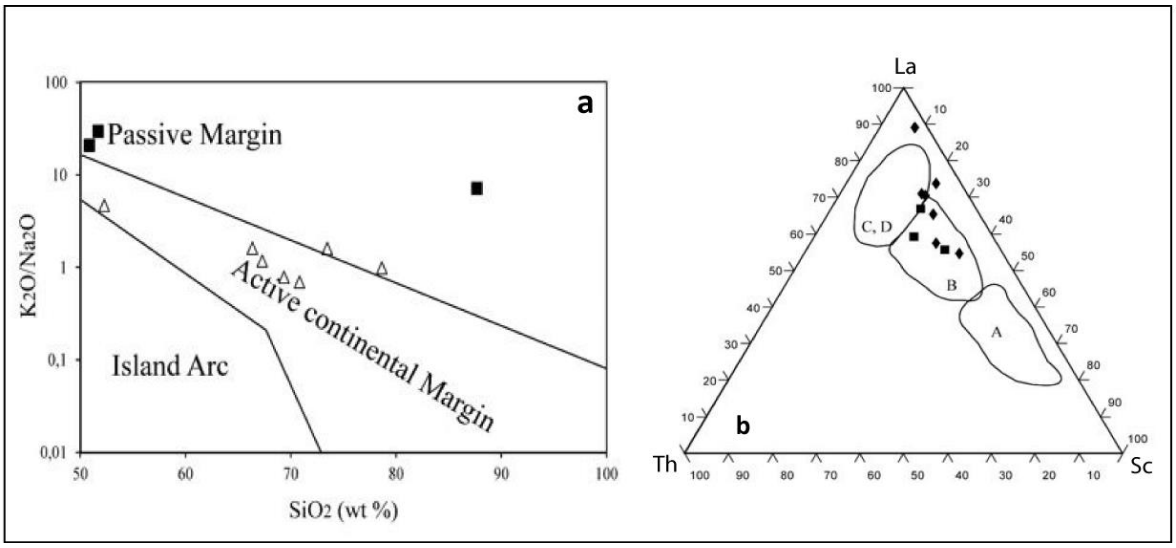

Fig 13: Plots of the major and trace element compositions from the studied materials on the tectonic setting discrimination diagrams [64]: (a). A: Oceanic Island Arc, B: Continental Island Arc, C: Active Continental Margin, D: Passive Margin [5]: (b)

6. Conclusion

This study was carried out on two alluvial profiles localised at the banks of an affluent of the Mayo Sina South West of Chad; twelve samples were subjected to a mineralogical and geochemical analyses (major, trace and REE). These analyses helped to determine the composition of the source rock and the tectonic setting.

The following conclusions can be drawn from this study:

1. The results obtained from the diffractometric analysis revealed that the total fraction is dominated by calcite in the whole rocks and quartz in the overlying materials. As for smectite, it is the major mineral present in clayey fraction;
2. in the two alluvial profiles, all the major elements trace and REE, except for CaO, Sr and Ni, increase from whole rocks to overlying materials;
3. the whole rocks on which are developed these two alluvial profiles are limestones;
4. the estimated geochemical parameters reveal that there is no genetic link between the overlying studied material and the limestones on which they are deposited. On the other hand, the results indicate that the analysed materials were derived from mainly felsic source rocks, with only minor contributions from basic sources and were deposited in a tectonically active continental margin and/or continental island arc setting. Lastly, the low CaO contents in sediments indicate the relative maturity of the most typical post-Archean shales, such as PAAS and NASC.

7. References

1. Abou El-Anwar EA, EL-Wekeil SS. Contribution to the provenance and paleoclimate of the Lower Paleozoic sandstones of Naqus Formation, Wadi Qena, Northern Eastern Desert: Integration of support petrography, mineralogy and geochemistry. Journal of Applied Sciences Research. 2013; 9(10):6529-6546.
2. Akarish, El-Gohary. Provenance and Source Area Weathering Derived from the Geochemistry of Pre-Cenomanian Sandstones, East Sinai, Egypt. Journal of Applied Sciences. 2011; 11:3070-3088.
3. Ali S, Stattegger K, Garbe-Schönberg D, Kraft S, Kuhnt W. The provenance of Cretaceous to Quaternary sediments in the Tarfaya basin, SW Morocco: Evidence from trace element geochemistry and radiogenic Nd–Sr isotopes. Journal of African Earth Sciences. 2014; 2014; 90:64-76.
4. Armstrong-Altrin JS, Lee YI, Verma SP, Ramasamy S. Geochemistry of sandstones from the Upper Miocene Kudankulam Formation, southern India: Implications for provenance, weathering and tectonic setting. Journal of Sedimentary Research. 2004; 74(2):285-297.
5. Bhatia MR. Plate tectonics and geochemical composition of sandstones. Journal of Geology. 1983; 91(6):611-627.
6. Bhatia MR, Crook KAW. Trace element characteristics of graywackes and tectonic setting discrimination of sedimentary basins. Contribut. Mineral.Petrol. 1986; 92(2):181-193.
7. Burnham OM, Schweyer J. Trace element analysis of geological samples by inductively coupled plasma mass spectrometry at the geoscience laboratories: revised capabilities due to improvements to instrumentation. Summary of field work and other activities. Ontario Geol. Surv. 2004; 54:1-20, Open File Report 6145
8. Condie KC. Chemical composition and evolution of the upper continental crust: contrasting results from surface samples and shales. Chemical Geology. 1993; 104:1-37.
9. Condie KC, Philip DNJ, Conway CM. Geochemical and detrital mode evidence for two sources of Early Proterozoic. Sedimentary Geology. 1992; 77:51-76.
10. Cox R, Lowe DR, Cullers RL. The influence of sediment recycling and basement composition on evolution of mudrock chemistry in the southwestern United States. Geochimica et Cosmochimica, 1995; 9(14):2919-2940.
11. Cullers RL, Chaudhuri S, Arnold B, Lee M, Wolf CW. Rare earth distributions in clay minerals and in clay-sized fraction of the lower Permian Havensville and Eskridge shales of Kansas and Oklahoma. Geochimica et Cosmochimica. 1975; 58(22):4955-4972.
12. Cullers RL, Chaudhuri C, Kilbane N, Koch R. REE in size fractions and sedimentary rocks of Pennsylvanian-

Permian age from the mid-continent of the USA. Geochimica et Cosmochimica. 1979; 43:1285-1301.
13. Cullers RL, Barrett T, Carlson R, Robinson B. Rare-Earth element and mineralogic changes in Holocene soil and stream sediment: a case study in the wet mountains region, Colorado, USA. Chemical Geology. 1987; 63:275-297.
14. Cullers RL. The controls on the major and trace element variation of shales, siltstones, and sandstones of Pennsylvanian-Permian age from uplifted continental blocks in Colorado to platform sediment in Kansas, USA. Geochimica et Cosmochimica. 1994; 58:4955-4972.
15. Cullers RL. The controls on the major- and trace-element evolution of shales, siltstones, and sandstones of Ordovician to Tertiary age in the Wet Mountains region, Colorado, USA. Chemical Geology, 1995; 123:107-131.
16. Cullers RL. The geochemistry of shales, siltstones and sandstones of Pennsylvanian–Permian age, Colorado, USA: implications for provenance and metamorphic studies. Lithos. 2000; 51:181-203.
17. Cullers RL. Implications of elemental concentrations for provenance, redox conditions, and metamorphic studies of shales and limestones near Pueblo, CO, USA: Chemical Geology. 2002; 191(4):305-327.
18. Cullers RL, Basu A, Suttner L. Geochemical signature of provenance in sand-size material in soils and stream sediments near the Tobacco Root batholith, Montan, USA. Chemical Geology. 1988; 70:335-348.
19. Cullers RL, Podkovyrov VN. Geochemistry of the Mesoproterozoic Lakhanda shales in southeastern Yakutia, Russia: implications for mineralogical and provenance control and recycling. Precambrian Research. 2000; 104:77-93.
20. Das BK, Al-Mikhlafi AS, Kaur P. Geochemistry of Mansar lake sediments, Jammu, India: implication for source-area weathering provenance, and tectonic setting. Journal of African Earth Sciences. 2006; 26:649-668.
21. Dickinson WR, Beard LS, Brakenridge GR, Erjavck JL, Ferguson RC, Inman KF. *et al.* Provenance of North American Phanerozoic sandstones in relation to tectonic setting. Geological Society of America, Bulletin. 1983; 94:225-235.
22. Dinelli E, Lucchini F, Mordenti A, Paganelli L. Geochemistry of Oligocene-Miocene sandstones of the northern Apennines (Italy) and evolution of chemical features in relation to provenance changes. Sedimentary Geology. 1999; 127:193-207.
23. Doumnang JC. Géologie des formations néoprotérozoïques du Mayo Kebbi (sud-ouest du Tchad): Apports de la pétrologie et de la géochimie, implications sur la géodynamique au Panafricain. Doctorat de 3ème Cycle, Université d'Orléans (France), 2006, 158.
24. Ekomane E, Bissé S, Ngueutchoua G, et Ngos III S. Contribution of major, trace and rare earth elements in the determination of sandstone and pelite source rocks in Bangue (Cameroon). Revue Cames. 2014; 02:2424-7235.
25. Feng R, et Kerrich R. Geochemistry of fine-grained clastic sediments in the Archean Abitibi greenstone belt, Canada: Implication for provenance and tectonic setting. Geochimica et Cosmochimica. 1990; 54:1061-1081.
26. Floyd PA, Winchester JA, Park RG. Geochemistry and tectonic setting of Lewisian clastic metasediments from the Early Proterozoic Loch Maree Group of Gairloch, N.W. Scotland: Precambrian Research. 1989; 45:203-214.
27. Fyffe LR, Pickerill RK. Geochemistry of Upper Cambrian-Lower Ordovician black shale along a northeastern Appalachian transect. Geological Society of America. 1993; 105:897-910.
28. Garver JI, Royce PR, Smick TA. Chromium and Nickel in shale of the Taconic Foreland; a case study for the provenance of fine-grained sediments with an ultramafic source. J Sedimentary Research. 1996; 66:100-106.
29. Graf DL. Geochemistry of carbonate sediments and sedimentary carbonate rocks, part III: minor element distribution. Division of the Illinois State geological survey. Circular. 1960; 301-76.
30. Gromet LP, Dymek RF, Haskin LA, Korotev RL. The North American Shale Composite: its compilation, major and trace element characteristics. Geochimica et Cosmochimica. 1984; 48:2469-2482.
31. Hayashi K, Fujisawa H, Holland H, Ohmoto H, Geochemistry of 1.9 Ga sedimentary rocks from northeastern Labrador, Canada: Geochimica et Cosmochimica. 1997; 61:4115-4137.
32. Hiscott RN. Ophiolitic source rocks for Taconic-age flysch: trace-element evidence. Geological Society of America. 1984; 95:1261-1267.
33. Isseini M. Croissance et différenciation crustale au Néoprotérozoïque Exemple du domaine panafricain du Mayo kebbi au Sud-Ouest du Tchad. Thèse/PhD. Univ. Henry Poincaré, Nancy I, 2011, 345.
34. Kasser MY. Evolution précambrienne de la région du Mayo Kebbi (Tchad). Un segment de la Chaîne Panafricaine. Doctorat de 3ème Cycle, Muséum d'Histoire Naturelle de Paris (France). 1995, 217.
35. Krauskopf KB. Economic Geology. 50th Aniversary. 1955, I-411.
36. Kronbergb I, et Nesbitt HW. Quantification of weathering soil geochemistry and soil fertility. Journal of Soil Sciences, 1981; 32:453-459.
37. López de Luchi MG, Cerredo ME, Siegesmund S, Steenken A, Wemmer K. Provenance and tectonic setting of the protoliths of the Metamorphic Complexes of Sierra de San Luis. Revista de la Asociación Geológica Argentina. 2003; 58(4):525-540.
38. López JMG, Bauluz B, Fernández-Nieto C, Olieten AY. Factors controlling the trace-element distribution in fine-grained rocks: the Albian kaolinite-rich deposits of the Oliete Basin (NE Spain). Chemical Geology. 2005; 214:1-19.
39. Madhavaraju J, Ramasamy S. Petrography geochemistry of Late Maastrichtian - Early Paleocene sediments of Tiruchirapalli Cretaceous, Tamil Nadu - Paleoweathering and provenance implications. Journal of the Geological Society of India. 2002; 59:133-142.
40. McDonough WF, Sun SS. The composition of the earth. Chemical Geology. 1995; 120:223-253.
41. McLennan SM. Rare earth elements in sedimentary rocks; influence of provenance and sedimentary processes, in Lipin BR, McKay GA. (eds.), Geochemistry and Mineralogy of Rare Earth Elements. Reviews in Mineralogy. 1989; 21:169-200.

42. McLennan SM, Taylor SR. Sedimentary rocks and crustal evolution: tectonic setting and secular trends. Journal of Geology. 1991; 99:1-21.
43. McLennan SM, Taylor SR, Eriksson KA. Geochemistry of Archean shales from the Pilbara Supergroup, Western Australia. Geochimica et Cosmochimica. 1983a; 47:1211-1222.
44. McLennan SM, Taylor SR, Kroner A. Geochemical evolution of Archean shales from South Africa 1. The Swaziland and Pongola Supergroups. Precambrian Research. 1983b; 22:93-124.
45. McLennan SM, Taylor SR, Mcculloch MT, Maynard JB. Geochemical and Nd-Sr isotopic composition of deep-seaturbidites: Crustal evolution and plate tectonic associations. Geochimica et Cosmochimica. 1990; 54:2015-2050.
46. McLennan SM, Taylor SR, McDaniel DK, Hanson GN. Geochemical approaches to sedimentation, provenance and tectonics, in processing controlling the composition of clastic sediments. In: Johnson MJ, Basu A. (Eds.). Geological Society of America. 1993; 284:21-40.
47. Nagarajan R, Madhavaraju J, Nagendra R, Armstrong-Altrin JS, Moutte J. Geochemistry of Neoproterozoic shales of the Rabanpalli Formation, Bhima Basin, Northern Karnataka, southern India: implications for provenance and paleoredox conditions. Revista Mexicana de Ciencias Geológicas. 2007; 24:150-160.
48. Ndjigui PD, Bilong P, Bitom D. Negative cerium anomalies in the saprolite zone of serpentinite lateritic profiles in the Lomié ultramafic complex, South East Cameroon. Journal of African Earth Sciences. 2009; 53:59-69.
49. Ndjigui PD, Beauvais A, Fadil-Djenabou S, Ambrosi JP. Origin and evolution of Ngaye River alluvial sediments, Northern Cameroon: Geochemical constraints. Journal of African Earth Sciences. 2014; 100:164-178.
50. Ndjigui PD, Ebah Abeng A. Ekomane SE, Nzeugang Nzeukou A, Ngo Mandeng S, Lindjeck Matoy M. Mineralogy and geochemistry of pseudogley soils and recent alluvial clastic sediments in the Ngog-Lituba region, Southern Cameroon: An implication to their genesis. JJournal of African Earth Sciences. 2015; 108:1-14.
51. Nesbitt HM, Markovics G, Price RC. Chemical processes affecting alkalis and alkaline earths during continental weathering. Geochimica et Cosmochimica. 1980; 44:1659-1666.
52. Nesbitt HW, et Young GM. Early Proterozoic climates and plate motions inferred from major element chemistry of lutites. Nature. 1982; 299:715-717.
53. Nesbitt HW, Young GM, McLennan SM, Keays RR. Effects of chemical weathering and sorting on the petrogenesis ofs Siliciclastic sediments, with implications for provenance studies. Journal of Geology. 1996; 104:525-542.
54. Nesbitt HW, Young GM. Petrogenesis of sediments in the absence of chemical weathering: effects of abrasion and sorting on bulk composition and mineralogy. Sedimentology, 1996; 43:341-358.
55. Nyakairu GWA, Koeberl C. Mineralogical and chemical composition and distribution of rare earth elements in clay-rich sediments from central Uganda. Geochemical Journal, 2001; 35:13-28.
56. Osae S, Asiedu DK, Banoeng-Yakubo B, Koeberl C, Dampare SB. Provenance and tectonic setting of Late Proterozoic Buem sandstones of southeastern Ghana: Evidence from geochemistry and detrital modes. Journal of African Earth Sciences. 2006; 44:85-96.
57. Paikaray SS, Banerjee S. Mukherji. Geochemistry of shales from the Paleoproterozoic to Neoproterozoic Vindhyan Super group: Implication on provenance, tectonic and paleoweathering. Journal of African Earth Sciences. 2008; 32:34-48.
58. Penaye J, Kröner A, Toteu SF, Van Schumus WR, Doumnang JC. Evolution of the Mayo Kebbi region as revealed by zircon dating: an early (ca. 740 Ma) Pan-African magmatic arc in south-western Chad. Journal of African Earth Sciences. 2006; 44:530-542.
59. Peterson JA. Geochemical Provenance of Clastic Sedimentary Rocks in the W estern Cordillera: Utah, Colorado, Wyoming, and Oregon. All Graduate Theses and Dissertations. 2009, 439.
60. Pouclet A, Vidal M, Doumnang JC, Vicat JP, Tchameni R. Neoproterozoic crustal evolution in Southern Chad: Pan-African ocean basin closing, arc accretion and late- to post-orogenic granitic intrusion. Journal of African Earth Sciences. 2006; 44:543-60.
61. Reimold WU, Koeberl C, Bishop J. Roter Kamm impact crater, Namibia: Geochemistry of basement rocks and breccias. Geochimica et Cosmochimica. 1994; 58:2689-2710.
62. Reynolds RC, Moore DW. X-ray Diffraction and the Identification and Analysis of Clay Minerals: New York Oxford University Press. 1989; 326.
63. Rollinson HR. Using geochemical data: Evaluation, presentation, interpretation. 1993 Longman 352.
64. Roser BP, Korsch RJ. Determination of tectonic setting of sandstone-mudstone suites using SiO2content and K2O/Na2O ratio. Journal of Geology. 1986; 94:635-650.
65. Roser BP, Korsch RJ. Provenance signatures of sandstone-mudstone suites determined using discriminant function analysis of major-element data. Chemical Geology. 1988; 67:119-139.
66. Rubinic V, Dum G, Husnjak S, Tadej N. Composition properties and formation of pseudogley on loess along a precipitation gradient in the Pannonian region of Croatia. Catena. 2014; 113:138-149.
67. Sawyer EW. The influence of source rock type, chemical weathering and sorting on the geochemistry of clastic sediments from the Quetico metasedimentary belt, Superiorprovince, Canada. Chemical Geology. 1986; 55:77-95.
68. Schwertmann U, Cornell RM. Iron Oxides in the Laboratory, Preparation and Characterization. VCH, Weinheim. 1991, 132.
69. Singh P, Major, trace and REE geochemistry on the Ganga river sediments: influence of provenance and sedimentary processes. Chemical Geology. 2009; 266:242-254.
70. Singh P, Rajamani V. REE geochemistry of recent clastic sediments from the source area weathering and sedimentary processes. Geochimica et Cosmochimica. 2001; 65:3093-3108.

71. Srodon J. Precise identification of illite/smectite interstratifications by X-ray powder diffraction. Clays and Clay Minerals. 1980; 28:401-411.
72. Taylor SR, McLennan SM. The Continental Crust: Its Composition and Evolution. Blackwell, Oxford. 1985, 312.
73. Wacrenier P, Laï-Garoua. Rapport de fin de mission, DMG Brazaville, 1953.
74. Wrafter JP, Graham JR. Short Paper: Ophiolitic detritus in the Ordovician sediments of South Mayo, Ireland. Journal of Geological Society. 1989; 146(2):213-215.
75. Wronkiewicz DJ, Condie KC. Geochemistry of Archean shales from the Witwatersrand Supergroup, South Africa: Source-area weathering and provenance. Geochimica et Cosmochimica. 1987; 51:2401-2416.
76. Wronkiewicz DJ, Condie KC. Geochemistry and mineralogy of sediments from the Ventersdorp and Transvaal Supergroups, South Africa: Cratonic evolution during the early Proterozoic. Geochimica et Cosmochimica. 1990; 54(2):343-354.